

Coherent atom-molecule oscillations in a Bose-Fermi mixture

M. L. Olsen, J. D. Perreault,* T. D. Cumby, and D. S. Jin

JILA, National Institute of Standards and Technology, and Department of Physics, University of Colorado, Boulder, Colorado 80309-0440, USA

(Received 10 October 2008; published 2 September 2009)

We create atom-molecule superpositions in a Bose-Fermi mixture of ^{87}Rb and ^{40}K atoms. The superpositions are generated by ramping an applied magnetic field near an interspecies Fano-Feshbach resonance to coherently couple atom and molecule states. Rabi- and Ramsey-type experiments show oscillations in the molecule population that persist as long as 150 μs and have up to 50% contrast. The frequencies of these oscillations are magnetic-field dependent and consistent with the predicted molecule binding energy. This quantum superposition involves a molecule and a pair of free particles with different statistics (i.e., bosons and fermions) and furthers exploration of atom-molecule coherence in systems without a Bose-Einstein condensate.

DOI: [10.1103/PhysRevA.80.030701](https://doi.org/10.1103/PhysRevA.80.030701)

PACS number(s): 34.80.Pa, 05.30.Jp, 05.30.Fk, 34.50.-s

Magnetic-field tunable Fano-Feshbach resonances in ultracold atom gases provide a quantum system that can couple atoms to a molecular bound state [1]. This coupling has been used to associate ultracold atoms into weakly bound molecules by adiabatically sweeping a magnetic field across a Fano-Feshbach resonance [2]. Quantum superpositions of molecules and *single* atom-pair states have also been created with these resonances, starting from a gas of bosonic atoms [3–7]. These atom-molecule superpositions are highly unusual in that they establish coherence between the chemically distinct states of a free-atom pair and a bound molecule. In experiments using identical bosons either in a Bose-Einstein condensate (BEC) [3] or confined pairs in a deep optical lattice potential [5], the atom-molecule oscillations are well described by a two-level model. However, observations of atom-molecule superpositions in thermal gases of bosons [4,8] extend coherent atom-molecule manipulation to more generic systems where the coherent atom-molecule oscillations involve a *continuum* of atom-pair states with different relative momenta. This raises the possibility of observing atom-molecule oscillations in a many-body system involving fermions, which is a subject that has been investigated theoretically [9–13]. In this Rapid Communication, we demonstrate atom-molecule superpositions in a Bose-Fermi mixture of ^{87}Rb and ^{40}K , where we use magnetic-field pulses near a Fano-Feshbach resonance to reveal coherent oscillations that persist for as long as 150 μs . Our work furthers exploration of atom-molecule coherence in non-BEC systems and provides the groundwork for possible future experiments. For example, the frequency, coherence time, and amplitude of such atom-molecule oscillations can be used to probe nonequilibrium dynamics and pairing processes in strongly interacting Bose-Fermi [10] and Fermi-Fermi [11–13] atom gases. Understanding atom-molecule coupling in this intrinsically multilevel system is also relevant to the goal of efficient molecule creation in trapped ultracold atom gases [14].

Efficient molecule creation using a Fano-Feshbach resonance requires an initial atom gas with high phase-space den-

sity [1,15]. We prepare an ultracold Bose-Fermi mixture of ^{87}Rb atoms in the $|f, m_f\rangle = |1, 1\rangle$ state and ^{40}K atoms in the $|9/2, -9/2\rangle$ state [16,17]. Here, f is the total atomic spin and m_f is the spin projection along the magnetic field. The atoms are confined in a far-off-resonance optical dipole trap formed by a single laser beam with a waist of 18 μm and a wavelength of 1090 nm. The gas mixture is evaporatively cooled by decreasing the power of the optical-trap beam. Following the evaporation, the optical-trap power is adiabatically increased, and the measured trap frequencies are 350 Hz for Rb and 490 Hz for K in the radial direction and 5.2 Hz for Rb and 8.1 Hz for K in the axial direction. In this trap, we have $N_{\text{Rb}} = 8 \times 10^4$ Rb atoms and $N_{\text{K}} = 2 \times 10^5$ K atoms at a temperature of 200 nK, which corresponds to 1.2 T_C and 0.3 T_F , where T_C is the critical temperature for Bose-Einstein condensation of the Rb gas and T_F is the Fermi temperature of the K gas.

Molecule detection is achieved with spin-selective absorption imaging using light tuned to the K $4S_{1/2}|9/2, -9/2\rangle \rightarrow 4P_{3/2}|11/2, -11/2\rangle$ cycling transition [18,19]. To avoid imaging unbound K atoms, we use a 30 μs pulse of rf tuned to the K Zeeman transition to transfer the atoms to the $|9/2, -7/2\rangle$ state with 99% efficiency. The molecules are unaffected since their binding energy of $h \times 140$ kHz (at 546.04 G) is larger than the spectral width of the rf pulse. The molecule cloud is imaged after 2 ms of expansion from the optical trap.

To characterize the atom-molecule coupling time scale, we first explored molecule creation via linear magnetic-field sweeps across the Fano-Feshbach resonance between Rb $|1, 1\rangle$ and K $|9/2, -9/2\rangle$ atoms at $B_0 = 546.76$ G [17]. The atoms are initially prepared by turning on an applied magnetic field of 542 G during the evaporation. The magnetic field is then increased to the high-field side of the resonance (547.2 G) after evaporation at a speed of $\dot{B}_{\text{fast}} = 140$ G/ms. Next, we sweep the magnetic field down through the resonance to 546.04 G and measure the number of molecules created by the sweep. The measured number of molecules created as a function of the magnetic-field ramp rate \dot{B} fits well to an exponential function $N_{\text{mol}} = N_{\text{max}}(1 - e^{-\beta/\dot{B}})$, where the two fit parameters are the saturated number of molecules for the slowest ramps $N_{\text{max}} = (2.9 \pm 0.3) \times 10^4$ and $1/e$ ramp

*johndp@jilau1.colorado.edu

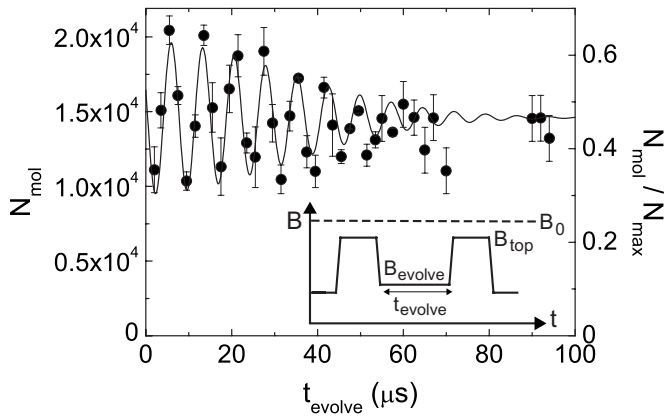


FIG. 1. Ramsey-type atom-molecule oscillations. The molecule number N_{mol} is shown as a function of the hold time at $B_{\text{evolve}}=546.08$ G. Here, we fit the data to $N_{\text{mol}}=Ae^{-t^2/(2\sigma^2)}\sin(2\pi\nu_{\text{osc}}t-\phi)+y_0$, which would describe, for example, oscillations that dephase due to inhomogeneous broadening. The fit gives an oscillation frequency $\nu_{\text{osc}}=(136.5\pm 1.3)$ kHz and rms damping time $\sigma=(32\pm 5)$ μs . The data fit equally well to an exponentially damped oscillation with a $1/e$ damping time of (43 ± 12) μs . (Inset) Schematic of magnetic-field pulse sequence.

speed $\beta=(26\pm 8)$ G/ms. For these data, the calculated peak number densities of the initial atom gas are $n_{\text{Rb}}^0=1.1\times 10^{13}$ cm^{-3} and $n_{\text{K}}^0=1.3\times 10^{13}$ cm^{-3} , for Rb and K atoms, respectively. The saturated molecule number N_{max} is 36% of N_{Rb} , which as the smaller atom number sets an upper limit on the number of molecules. N_{max} is significantly lower than the prediction of a phenomenological model that has been shown to successfully predict molecule conversion [15,19,20]. This may be due to collisional losses or heating near the resonance.

To create atom-molecule superpositions we use nonadiabatic ramps with speeds that are fast compared to β , similar in technique to references [3,5]. We first consider atom-molecule coherence far from the resonance, where we use a double-pulse experiment that is analogous to Ramsey's method of separated oscillatory fields [1,21,22]. A schematic of the magnetic-field ramps is shown in the inset of Fig. 1. The two pulses toward resonance couple the atom and molecule states. The duration and magnetic field of the pulses are empirically optimized for maximum amplitude oscillations in the molecule population. The pulse sequence begins after a slow (3 G/ms) ramp to 545.80 G and consists of two trapezoidal pulses with 15 μs holds at $B_{\text{top}}=546.58$ G, separated by a variable hold time t_{evolve} at B_{evolve} . The outer ramps have speeds of \dot{B}_{fast} , while the inner ramps have speeds of $(B_{\text{top}}-B_{\text{evolve}})/5$ μs [23]. At B_{top} , the calculated molecule size is $1800a_0$, which is comparable to the typical distance between nearest-neighbor Rb and K atoms, which is approximately $n^{-1/3}=10\,500a_0$. Here, $n=(1/N_{<})\int n_{\text{K}}(r)n_{\text{Rb}}(r)d^3r$, where n_{K} and n_{Rb} are the number densities of K and Rb, respectively, and $N_{<}$ is the number of atoms in the species with fewer atoms.

Figure 1 shows the measured molecule number after a double-pulse sequence with $B_{\text{evolve}}=546.08$ G. The right-

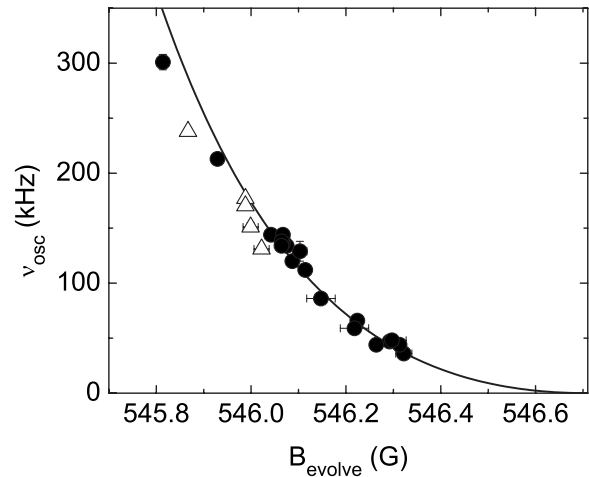


FIG. 2. Magnetic-field dependence of the measured molecule number oscillation frequency in Ramsey-type double-pulse experiments. The circles (\bullet) correspond to double-pulse experiments performed with the atoms confined in the optical trap, while the triangles (Δ) represent experiments performed after 1 ms of expansion from the trap. The solid line is a fit to the universal prediction for molecule binding energy [24] for the data above 546 G [25].

hand axis shows the molecule number N_{mol} normalized by N_{max} . The molecule number shows clear oscillations as a function of t_{evolve} as expected for a coherent atom-molecule superposition. We observe a peak-to-peak amplitude of 10^4 molecules, which is 13% of N_{Rb} .

As further evidence that these oscillations are due to atom-molecule superpositions, we have measured the oscillation frequency for various values of B_{evolve} and find that the frequency corresponds to the predicted binding energy of the molecules. Figure 2 shows the measured oscillation frequency ν_{osc} as a function of the hold magnetic field B_{evolve} . The solid curve is a fit to the universal prediction for the molecule binding energy near the resonance, $E_b=\hbar^2/[2\mu_{\text{KRb}}(a-\bar{a})^2]$ [24]. Here, μ_{KRb} is the ^{40}K and ^{87}Rb reduced mass, $\bar{a}=68.8a_0$, and $a=a_{\text{bg}}[1-\Delta/(B-B_0)]$ with $a_{\text{bg}}=-185a_0$ [26]. From the fit, we extract the resonance position $B_0=(546.71\pm 0.01)$ G and width $\Delta=(-3.34\pm 0.05)$ G, in agreement with Ref. [19].

Figure 2 also includes data taken at significantly lower atom number densities. Here, we lower the density of the atoms by turning off the optical trap and allowing the gas to expand before applying the magnetic-field pulses. For these data, at the end of evaporation, we have 1×10^6 Rb atoms and 6×10^5 K atoms at 1200 nK in an optical trap with radial trapping frequencies of 690 and 970 Hz for Rb and K, respectively. The temperature corresponds to $T/T_C=1.6$ for Rb and $T/T_F=0.7$ for K. The triangles in Fig. 2 correspond to experiments performed after 1 ms of expansion using a hold time of 50 μs at the top of the optimized pulses. After 1 ms of expansion, the peak densities are $n_{\text{Rb}}^0=3\times 10^{12}$ cm^{-3} and $n_{\text{K}}^0=7\times 10^{11}$ cm^{-3} . By performing linear magnetic-field sweeps as discussed earlier, we find $N_{\text{max}}=(9.2\pm 0.6)\times 10^4$, which is 15% of N_{K} , and $\beta=(9.1\pm 1.0)$ G/ms.

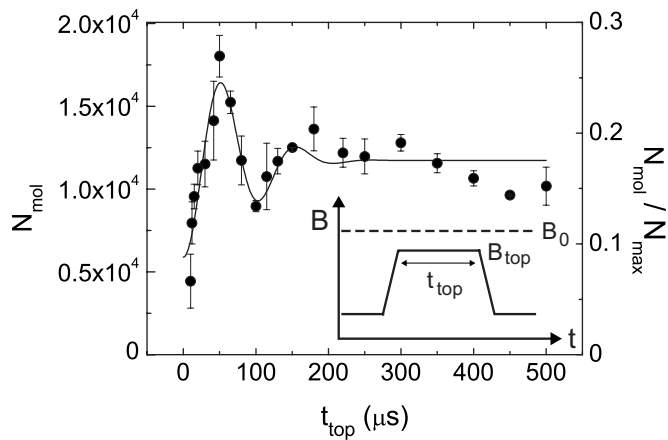


FIG. 3. Rabi-type atom-molecule oscillations. The measured molecule number is shown as a function of the hold time for a single pulse where B_{top} was 546.51 G. The line is a fit to $N_{\text{mol}} = A e^{-t^2/(2\sigma^2)} \cos(2\pi\nu_{\text{osc}}t) + y_0$, yielding a frequency $\nu_{\text{osc}} = (9.3 \pm 0.5)$ kHz and rms damping time $\sigma = (80 \pm 20)$ μs . If we fit the data to an exponentially damped oscillation, the $1/e$ damping time is (80 ± 30) μs . (Inset) Schematic of the magnetic-field pulse.

For values of B_{evolve} that approach the resonance, the double magnetic-field pulse shown in the inset to Fig. 1 would begin to resemble a single pulse. Therefore, to study atom-molecule oscillations at magnetic fields closer to the resonance, we employ single magnetic-field pulses that realize a Rabi-type experiment. Previously, oscillations were seen in single-pulse experiments with a single species of bosons [3–5]. However, in the BEC system, oscillations in these Rabi-type experiments proved more difficult to observe than those in double-pulse experiments [3]. In our case, we find that we are only able to observe oscillations in a single-pulse experiment at the lower densities enabled by expansion of the gas. For the higher-density trapped gas, the coherent atom-molecule oscillations seen in the double-pulse experiments prove that there must be coherent evolution during each single pulse; however at these densities it appears that the coherence time at B_{top} is too short to permit the observation of even one full Rabi oscillation.

A schematic of a single pulse is shown in the inset of Fig. 3. The magnetic field is ramped from 545.80 G to B_{top} , held for a time t_{top} , and ramped back down, with both ramps having speeds of \dot{B}_{fast} . Figure 3 shows the measured molecule population in the expanded gas after a single pulse to $B_{\text{top}} = 546.51$ G as a function of the hold time t_{top} . Defining the contrast as the $t_{\text{top}} = 0$ amplitude $|A|$ divided by the final level of the damped oscillation y_0 , we measure a contrast of 0.5 ± 0.2 .

In optimizing the peak-to-peak amplitude of the oscillations in the molecule population, we find that the amplitude depends on the value of B_{top} as shown in Fig. 4(a). In addition, as B_{top} is increased, we observe fewer oscillations before they damp out, and for the data above $B_{\text{top}} = 546.6$ G, only one period of the oscillation is observed. Therefore, we define the peak-to-peak amplitude as the difference in molecule number between the first maximum and the subsequent

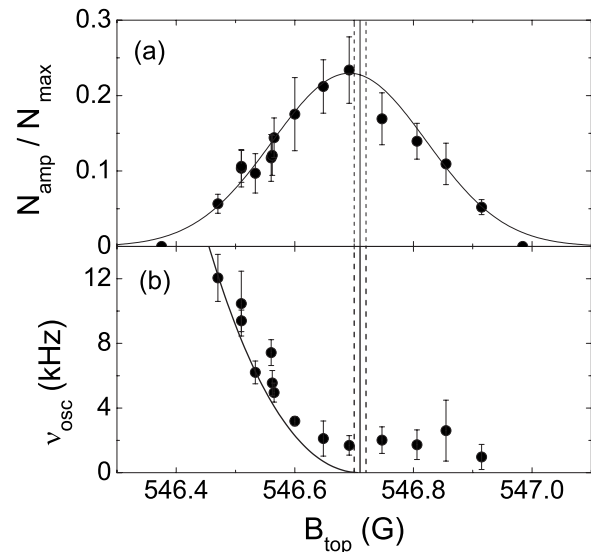


FIG. 4. Magnetic-field dependence of the (a) peak-to-peak amplitude and (b) frequency of the single-pulse oscillations. The solid line in (a) is a Gaussian fit to the data, while the solid line in (b) is the universal prediction for the molecule binding energy from Fig. 2. The vertical lines represent the fitted Fano-Feshbach resonance position and uncertainty from Fig. 2.

minimum. The amplitude of the oscillations is peaked near the Fano-Feshbach resonance where we observe a peak-to-peak amplitude that is 23% of N_{max} . At $B_{\text{top}} = 546.47$ G, the oscillation amplitude drops to 6% of N_{max} . Here, the calculated molecule size is $1100a_0$, which is 5% of the typical distance between nearest-neighbor K and Rb atoms of $23\,700a_0$.

The frequency of the Rabi-type oscillations also depends on B_{top} as shown in Fig. 4(b). Below the resonance, the measured frequency agrees with the prediction for the molecule binding energy. Above 546.6 G, the frequency obtained by fitting to a Gaussian-damped oscillation saturates, which can be understood in terms of a *multilevel* Landau-Zener diagram [27,28]. This is in contrast to the *two-level* atom-molecule system explored by Syassen *et al.* [5], in which the measured frequency as a function of magnetic field is symmetric about the resonance. In our experiment, the molecule state can couple to many closely spaced atom-pair energy levels [27,28]. The energy spacing of these levels could set a lower limit on the oscillation frequency. We note that the observed saturation frequency of (1.7 ± 0.8) kHz is on the order of the expected many-body level spacing of 0.6 kHz [27].

The results of the single-pulse experiments can be used to infer the best pulses for double-pulse experiments. Maximum contrast should be achieved by using pulses where the hold time at B_{top} gives one quarter cycle of the single-pulse oscillation, which is analogous to a $\pi/2$ pulse in Ramsey's experiments [29]. In fact, we find that the empirically optimized pulse sequence for the expanded clouds corresponds to this condition.

For both the single-pulse and double-pulse experiments, we observe damping of the atom-molecule oscillations. Because the time-averaged number of molecules does not decrease, this damping is not due to a loss of molecules. In-

deed, we measure molecule lifetimes longer than a millisecond over the range of densities and fields probed [30]. The loss of contrast is instead likely caused by dephasing due to a range of oscillation frequencies among the pairs. For our Bose-Fermi gas mixture, a range of oscillation frequencies is expected because there is a spread in the relative kinetic energy of the pairs, E_{rel} . The oscillation frequency for a given atom pair is $\nu_{\text{pair}} = (E_b + E_{\text{rel}})/h$. As a rough estimate of this damping time, we have performed a semiclassical Monte Carlo calculation of the expansion and find that the distribution of relative kinetic energies for nearest-neighbor Rb and K atoms would give a $75 \mu\text{s}$ $1/e$ damping time. While this agrees well with the data shown in Fig. 3, we observe faster damping rates for oscillations farther from the Fano-Feshbach resonance. This suggests that a technical source of dephasing, such as a spatial inhomogeneity in the applied magnetic field, may be important. Given the quadratic dependence of E_b on magnetic field, a spatial variation in magnetic field would result in more rapid dephasing for larger magnetic-field detuning from the Fano-Feshbach resonance. Future efforts will focus on minimizing technical

causes of dephasing and investigating the intrinsic dephasing due to the relative kinetic energies of the atom pairs.

In conclusion, we have observed atom-molecule Rabi- and Ramsey-type oscillations using a mixture of bosons and fermions. We do not start with a BEC or prepare the system in a single energy state [3,5] but rather extend previous work by coherently coupling atoms with a distribution of energies [4,8] to a fermionic molecule state. We observe relatively large amplitude oscillations that persist up to $150 \mu\text{s}$. The frequency, coherence time, and amplitude of these atom-molecule oscillations may provide a unique way to probe the many-body behavior of a strongly interacting Bose-Fermi mixture [10]. Additionally, it will be interesting to explore decoherence mechanisms for this non-Bose condensed superposition.

We thank C. H. Greene, E. A. Cornell, and the JILA BEC group for useful discussions. We acknowledge funding from NIST and NSF. J.D.P. acknowledges support from a NRC Research Associateship Award at NIST.

-
- [1] T. Köhler, K. Góral, and P. S. Julienne, *Rev. Mod. Phys.* **78**, 1311 (2006).
- [2] C. A. Regal, C. Ticknor, J. L. Bohn, and D. S. Jin, *Nature (London)* **424**, 47 (2003).
- [3] E. A. Donley, N. R. Claussen, S. T. Thompson, and C. E. Wieman, *Nature (London)* **417**, 529 (2002).
- [4] S. T. Thompson, E. Hodby, and C. E. Wieman, *Phys. Rev. Lett.* **95**, 190404 (2005).
- [5] N. Syassen, D. M. Bauer, M. Lettner, D. Dietze, T. Volz, S. Durr, and G. Rempe, *Phys. Rev. Lett.* **99**, 033201 (2007).
- [6] K. Winkler, G. Thalhammer, M. Theis, H. Ritsch, R. Grimm, and J. H. Denschlag, *Phys. Rev. Lett.* **95**, 063202 (2005).
- [7] C. Ryu, X. Du, E. Yesilada, A. M. Dudarev, S. Wan, Q. Niu, and D. J. Heinzen, e-print arXiv:cond-mat/0508201.
- [8] R. Dumke, J. D. Weinstein, M. Johanning, K. M. Jones, and P. D. Lett, *Phys. Rev. A* **72**, 041801(R) (2005).
- [9] O. Dannenberg, M. Mackie, and K.-A. Suominen, *Phys. Rev. Lett.* **91**, 210404 (2003).
- [10] M. Wouters, J. Tempere, and J. T. Devreese, *Phys. Rev. A* **67**, 063609 (2003).
- [11] A. V. Andreev, V. Gurarie, and L. Radzihovsky, *Phys. Rev. Lett.* **93**, 130402 (2004).
- [12] R. A. Barankov and L. S. Levitov, *Phys. Rev. Lett.* **93**, 130403 (2004).
- [13] J. von Stecher and C. H. Greene, *Phys. Rev. Lett.* **99**, 090402 (2007).
- [14] K. K. Ni, S. Ospelkaus, M. H. G. de Miranda, A. Pe'er, B. Neyenhuis, J. J. Zirbel, S. Kotochigova, P. S. Julienne, D. S. Jin, and J. Ye, *Science* **322**, 231 (2008).
- [15] E. Hodby, S. T. Thompson, C. A. Regal, M. Greiner, A. C. Wilson, D. S. Jin, E. A. Cornell, and C. E. Wieman, *Phys. Rev. Lett.* **94**, 120402 (2005).
- [16] J. Goldwin, S. Inouye, M. L. Olsen, B. Newman, B. D. DePaola, and D. S. Jin, *Phys. Rev. A* **70**, 021601(R) (2004).
- [17] S. Inouye, J. Goldwin, M. L. Olsen, C. Ticknor, J. L. Bohn, and D. S. Jin, *Phys. Rev. Lett.* **93**, 183201 (2004).
- [18] C. Ospelkaus, S. Ospelkaus, L. Humbert, P. Ernst, K. Sengstock, and K. Bongs, *Phys. Rev. Lett.* **97**, 120402 (2006).
- [19] J. J. Zirbel, K.-K. Ni, S. Ospelkaus, T. L. Nicholson, M. L. Olsen, P. S. Julienne, C. E. Wieman, J. Ye, and D. S. Jin, *Phys. Rev. A* **78**, 013416 (2008).
- [20] S. B. Papp and C. E. Wieman, *Phys. Rev. Lett.* **97**, 180404 (2006).
- [21] N. F. Ramsey, *Phys. Rev.* **78**, 695 (1950).
- [22] K. Góral, T. Köhler, and K. Burnett, *Phys. Rev. A* **71**, 023603 (2005).
- [23] The maximum magnetic-field ramp speed is limited by the bandwidth of the servo. The time-dependent B field, measured using rf spectroscopy on the K atoms, is within 40 mG of the desired field over the duration of the pulse.
- [24] G. F. Gribakin and V. V. Flambaum, *Phys. Rev. A* **48**, 546 (1993).
- [25] The cutoff of 546 G in the fit was determined by a comparison of the universal prediction for molecule binding energy to a multichannel calculation, obtained through private communication with P. S. Julienne.
- [26] F. Ferlaino, C. D'Errico, G. Roati, M. Zaccanti, M. Inguscio, G. Modugno, and A. Simoni, *Phys. Rev. A* **74**, 039903(E) (2006).
- [27] B. Borca, D. Blume, and C. H. Greene, *New J. Phys.* **5**, 111 (2003).
- [28] P. S. Julienne, E. Tiesinga, and T. Kohler, *J. Mod. Opt.* **51**, 1787 (2004).
- [29] N. F. Ramsey, *Rev. Mod. Phys.* **62**, 541 (1990).
- [30] J. J. Zirbel, K.-K. Ni, S. Ospelkaus, J. P. D'Incao, C. E. Wieman, J. Ye, and D. S. Jin, *Phys. Rev. Lett.* **100**, 143201 (2008).